

Ion-Optical Design of a Mass Spectrometer for Analyzing Complex Molecules during Fast Flybys

Janis Schertenleib
University of Bern, Space Research
and Planetary Sciences
Sidlerstrasse 5, 3012 Bern
janis.schertenleib2@unibe.ch

Rico G. Fausch
University of Bern, Space Research
and Planetary Sciences
Sidlerstrasse 5, 3012 Bern
rico.fausch@unibe.ch

Peter Wurz
University of Bern, Space Research
and Planetary Sciences
Sidlerstrasse 5, 3012 Bern
peter.wurz@unibe.ch

Abstract— Future deep space missions visiting the moons Io or Enceladus plan to analyze these objects' tenuous upper atmospheres to detect complex (bio-) molecules. Furthermore, the sampling of eruption plumes could reveal detailed information on subsurface chemical and biological processes. However, many planned or proposed mission designs foresee high flyby velocities on these objects, typically exceeding 5 km/s and amounting up to 20 km/s, referred to as hypervelocity. These high relative encounter velocities with respect to the atmospheric gas complicate the detection and unambiguous identification of complex molecules using state-of-the-art mass spectrometers due to molecular fragmentation caused by hypervelocity impact induced bond-dissociation. Additional ambiguity is caused by the constant presence of gas outgassing from the spacecraft, as this introduces an undesired background to the measurements that challenges the assignment of each compound to its origin, i.e., the spacecraft or the exosphere. Here, we present the ion-optical design of a time-of-flight mass spectrometer, referred to as OpenTOF, using a novel gas inlet system where species enter the mass analyzer on a direct trajectory, without any surface contact, at velocities up to 20 km/s. This prevents hypervelocity impact induced fragmentation. Furthermore, the novel gas inlet system causes both the mass resolution of the instrument and the flight times of ions to depend on the velocity with which the species enter the ion-optical system. As a consequence, OpenTOF provides the unique capability to separate species originating from spacecraft outgassing from the gas originating from the object's exosphere. The optimized ion-optical system design covers a mass range of m/z 1 to 800 and provides a mass resolution up to $m/\Delta m = 1,000$ (full width at half maximum). OpenTOF is comparable in size (250 mm characteristic length), weight (3.2 kg + 3 kg shielding), and performance (6 decades dynamic range in 10 s, about 12 W) to the Neutral and Ion Mass spectrometer (NIM) launched on-board ESA's Jupiter Icy Moons Explorer (JUICE/ESA), thanks to heritage of its electronics. Thanks to its two novel features, a contactless ion inlet at hypervelocity, and the capability to separate spacecraft background, OpenTOF will be able to perform highly reliable and unambiguous composition measurements of tenuous upper atmospheres and plumes, providing key data to improve our understanding of the status, origin, and evolution of the Solar System.

TABLE OF CONTENTS

1. INTRODUCTION.....	1
2. ION-OPTICAL SYSTEM.....	3
3. SPACECRAFT BACKGROUND SEPARATION.....	3
4. CONCLUSION.....	5
REFERENCES.....	6
BIOGRAPHY.....	7

1. INTRODUCTION

Mass spectrometers deployed on-board spacecraft are used to gather in-situ quantitative composition measurements of major and minor species present in planetary atmospheres with high sensitivities, unreachable by remote sensing techniques. While the most abundant species in planetary atmospheres are light molecules such as CH₄, H₂O, N₂, or CO₂ as well as atomic noble gasses, modern mass spectrometers aim to analyze also heavier trace components. Especially on planets and moons with volcanic activity, cryovolcanic activity, or plumes, such as Io, Europa, or Enceladus, the plumes are expected to contain complex molecules. In case of plumes putatively originating from an underlying ocean there is potential biologic relevance of some species, originating on or below the surface [1], [2]. Flying through these plumes and analyzing the material with a sensitive mass spectrometer could therefore provide valuable insights into the chemistry present under the surface. For such flyby maneuvers, many modern mission concepts foresee relative encounter velocities exceeding 5 km/s and up to 19 km/s [3], [4], which we will refer to as hypervelocity.

High relative encounter velocities with respect to the analyzed atmospheric gas are a major design driver for spaceborne mass spectrometers. Reference [5] discusses the implications of hypervelocity flybys and the resulting design drivers in detail. As the time spent near closest approach of the object is usually limited to a few minutes or even seconds, the acquisition speed of the instrument critically translates to

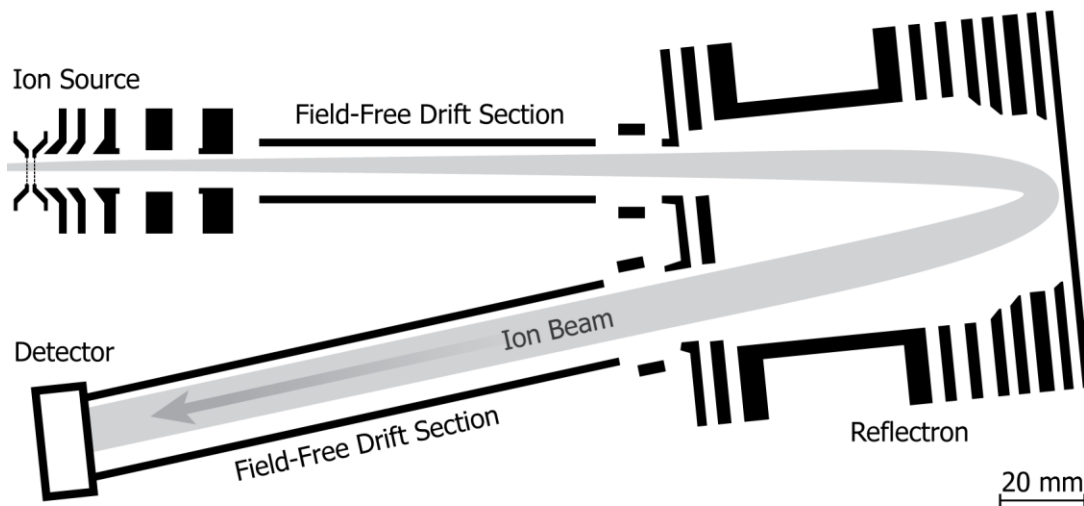


Figure 1. Schematic cross-section of OpenTOF's ion-optical system. The ion beam trajectory is based on SIMION simulations.

the amount of data that can be gathered [5]. Over the past decades, this quest has led to the advent of time-of-flight (TOF) mass spectrometers [6]–[8] that are able to record full mass spectra continuously and output a full mass spectrum about every 100 ms. In contrast, the previously favored quadrupole and magnetic sector instruments need to perform slow mass scans over tens of seconds or even minutes [9], [10]. However, the need for high acquisition speed is not the only consequence of high relative encounter velocities. Since the kinetic energy of the gas (in the rest frame of the spacecraft) scales with the square of the encounter velocity, the energies of particles in the gas beam are much higher than those handled in ground-based instruments. Current instruments like the Neutral and Ion Mass Spectrometer (NIM) launched on-board ESA's Jupiter Icy Moons Explorer (JUICE) in 2023 use two different gas inlet systems to handle the high velocity gas influx – the closed source and the open source [11]–[14].

In closed-source mode [12]–[14], the gas to be analyzed is collected in an antechamber before it reaches the mass analyzer. During multiple collisions with the inside walls the gas loses its high kinetic energy until it reaches thermal equilibrium with the chamber walls. This technique has the advantage that it can be used at very high relative encounter velocity, for example up to 70 km/s as anticipated by the mass spectrometer on board ESA's Comet Interceptor spacecraft [15]. Furthermore, the density inside the antechamber is enhanced with respect to ambient density [16], further increasing the sensitivity of the instrument. On the downside, the energetic impact of ions onto the walls of the antechamber will lead to unwanted fragmentation of molecules, referred to as hypervelocity impact (HVI) induced fragmentation. While this process is not yet fully understood, both experimental and simulation studies have reported upper limits for onset of HVI induced fragmentation for bare organic molecules at impact velocities around 6 km/s [17], [18]. Other than for the molecular fragmentation caused by

the electron ionization (EI) method, which is used in many systems including NIM, the fragmentation patterns from HVI induced fragmentation are not known well enough to enable reliable reconstruction of parent species. Especially where both fragmentation mechanisms concur, the result may be an indistinguishable superposition of primary species, EI and HVI fragments. Furthermore, currently no test facilities exist that are capable of producing the hypervelocity neutral gas beams required for the calibration of instruments and verification of theoretical models [5]. Therefore, the interpretation of measurements of complex molecules from closed-source instruments is difficult.

In open-source mode [12] species are first ionized and then led to the mass analyzer by deflecting them by 90° using electrostatic means. This technique avoids any surface contact of the analyzed gas and therefore also the ambiguity introduced by HVI induced fragmentation. However, given the high kinetic energies of heavy molecules at high relative encounter velocities, the high voltages required to maintain the focus of the ion beam limit this gas inlet type to relative encounter velocities of up to about 5 km/s.

HVI induced fragmentation is not the only source of ambiguity in spaceborne mass spectrometry. Even after years in space, outgassing from the spacecraft originating, for example, from printed circuit boards, structure, fuel, lubricants, and other payloads inevitably contribute to a permanent gas cloud around the spacecraft. This has been known to cause degraded performance especially for optical systems, for example on the Cassini-Huygens mission [19]. For mass spectrometers, with reported number densities of about 10^5 cm^{-3} even after long durations in space this outgassing interferes with the ambient gas of interest to be measured and therefore limits the instrument's sensitivity to detect trace species [20]. Consequently, the capability of performing unambiguous mass spectrometric measurements during hypervelocity flybys is currently compromised by

both HVI induced fragmentation and spacecraft outgassing.

Here, we present the ion-optical design of a TOF mass spectrometer with a novel gas inlet system that enables reliable and unambiguous measurements at relative encounter velocities up to 20 km/s. This instrument overcomes HVI fragmentation by design and provides possibilities to separate species originating the spacecraft from the local exosphere.

2. ION-OPTICAL SYSTEM

The ion-optical system (IOS) of this novel instrument, referred to as OpenTOF, has been described in detail by Fausch et al. [21]. Briefly summarized, OpenTOF employs a novel gas inlet system, referred to as the direct open source (DOeS), which requires neither a thermalizing antechamber nor orthogonal extraction [22]. Thus, both the problems of HVI induced fragmentation and the high voltages needed for orthogonal deflection are avoided. As depicted schematically in Figure 1, the ambient gas enters the ion-optical system on a straight trajectory. A thermionic cathode installed between the first two electrodes provides electron ionization [23]. Subsequently, a positive voltage pulse of nominally +600 V is applied to the entrance electrode, accelerating all ions momentarily present in the ionization region, and starting the flight time measurement. The ion beam is focused by a series of electrostatic lenses. After a field-free drift section, where ions of different masses separate along their trajectory, an ion mirror or reflectron [24] provides energy and spatial focusing. Passing a second field-free drift section the ions are guided onto a microchannel plate (MCP) detector providing flight time stop signals. Since each ion's flight time depends on its mass-to-charge ratio m/z , the recorded flight time spectrum can be converted to a mass spectrum.

All ambient gas species entering the DOeS system have a common on-axis velocity component corresponding to the relative encounter velocity between the spacecraft and the ambient medium, v_{rel} . Consequently, in contrast to the classical TOF mass spectrometer, the ions' kinetic energy inside the mass analyzer E depends on the ion mass m :

$$E = \frac{m}{2} v_{\text{rel}}^2 + E_{\text{acc}} + E_{\text{th}}, \quad (1)$$

where E_{acc} is the kinetic energy transferred to the ions by the extraction pulse, and E_{th} is the thermal energy. The additional mass dependent energy component is significant; for an ion at the high end of OpenTOF's mass range, m/z 800, and $v_{\text{rel}} = 20$ km/s it amounts to about 1.6 keV, much larger than the other two components. Since the mean kinetic energy for ions of equal m/z is still identical, the flight time spectrum still maps to a mass spectrum. However, the ion mirror of the DOeS type mass spectrometer must be able to provide energy focusing for a large range of mean kinetic energies. Our ion-optical simulations show that the ion mirror designed for OpenTOF can provide adequate energy focusing for a mass range up to m/z 1,000 at 10 km/s [5]. At higher relative

encounter velocities, a second voltage pulse is applied to the last ion source electrode to reduce the energy spread of the ions [21].

The dependence of E on v_{rel} is also significant. While the parameter v_{rel} is the same for all ions entering the instrument at the same time from the ambient medium, v_{rel} is zero for species originating in the outgassing gas cloud surrounding the spacecraft. The kinetic energy of these species inside the IOS therefore differs from the energy of the ambient gas influx, influencing their trajectories and flight times. In the following section, we will discuss how this can be used to distinguish the interfering outgassing background from the target measurements.

3. SPACECRAFT BACKGROUND SEPARATION

Since the range of mean ion energies depends strongly on v_{rel} , the IOS must be tuned for optimal performance to adapt to the current relative velocity to the surrounding medium. This is done by optimizing the values of the voltages applied to the IOS's electrodes, referred to as a voltage set, and can be automated [25]. We have performed ion-optical simulations using the SIMION® software to optimize voltage sets for high mass resolution $m/\Delta m$ at a purely thermal ion velocity distribution ($v_{\text{rel}} = 0$ km/s), as well as for relative encounter velocities of 10 km/s and 20 km/s. For the thermal energy component E_{th} a Maxwell-Boltzmann distribution at 1,000 K is assumed in all three cases. As depicted in Figure 2, the mass resolution for ions of m/z 1 start at $m/\Delta m \approx 250$ (full width at half maximum, FWHM), increasing rapidly for higher m/z before plateauing between $m/\Delta m = 1,000$ and 1,250. Unitary mass resolution, the minimum mass resolution required to distinguish adjacent integer masses, is achieved over the full nominal mass range of m/z 1 to 800, with good margin.

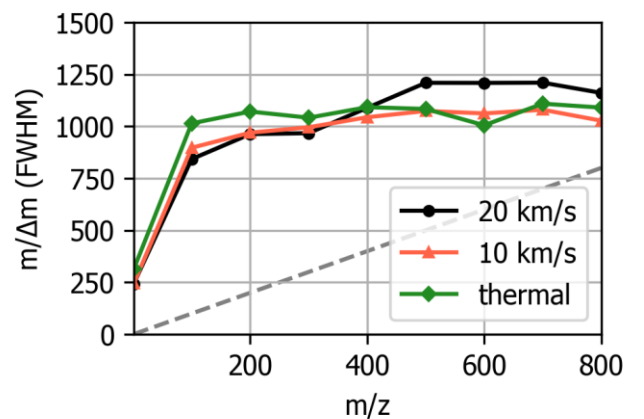


Figure 2. Mass resolution of OpenTOF as derived from SIMION simulations using voltage sets optimized for various relative encounter velocities. The dashed gray line indicates unitary mass resolution.

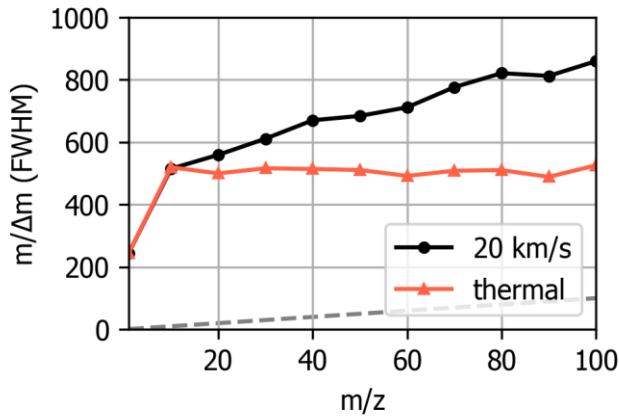


Figure 3. Mass resolution of OpenTOF as derived from SIMION simulations using a voltage set optimized for a relative encounter velocity of 20 km/s. The dashed gray line indicates unitary resolution.

While the mass resolution is almost the same for all three considered cases (thermal, 10 km/s, and 20 km/s) when using properly optimized voltage sets, species entering the instrument at a different velocity than the voltage set was optimized for generally exhibit diminished mass resolution. Figure 3 shows the mass resolution of species entering the instrument at 20 km/s and thermal velocity respectively when using a voltage set optimized for 20 km/s. Here, we only show a reduced mass range of m/z 1 to 100, since this is the range where significant outgassing contamination must be expected [20]. Because the spacecraft velocity term in Equation (1) scales with m as well as v_{rel} , the mass resolution for the two cases is indistinguishable up to m/z 10. Starting at m/z 20, however, the mass resolution of the thermal population plateaus at $m/\Delta m \approx 500$, whereas the mass resolution of the 20 km/s population continues increasing. In a mass spectrum, thermal ion signals, such as the ones originating from spacecraft outgassing, can therefore be

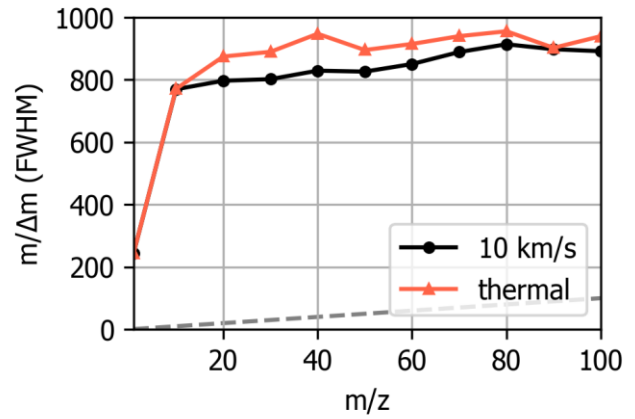


Figure 4. Mass resolution of OpenTOF as derived from SIMION simulations using a voltage set optimized for a relative encounter velocity of 10 km/s. The dashed gray line indicates unitary resolution.

distinguished from ambient signals by their broader peak widths. The contrast between the mass resolutions of species encountered at different relative velocities strongly depends on the difference of the squares of these velocities. As apparent in Figure 4, the difference in mass resolutions between species encountered at 10 km/s and thermal velocities, when using a voltage set optimized for 10 km/s, is minuscule.

Of course, one must expect that the ambient gas and the outgassing background will contribute ions of identical m/z summing up in the mass spectrum. If the contrast in mass resolution between the two contributors is large enough and the peak shapes are well known, the two contributions can then still be separated using peak fitting routines. However, a difference in mass resolution is not the only result of the ion energy depending on encounter velocity. The high initial on-axis velocity of the ions streaming into the

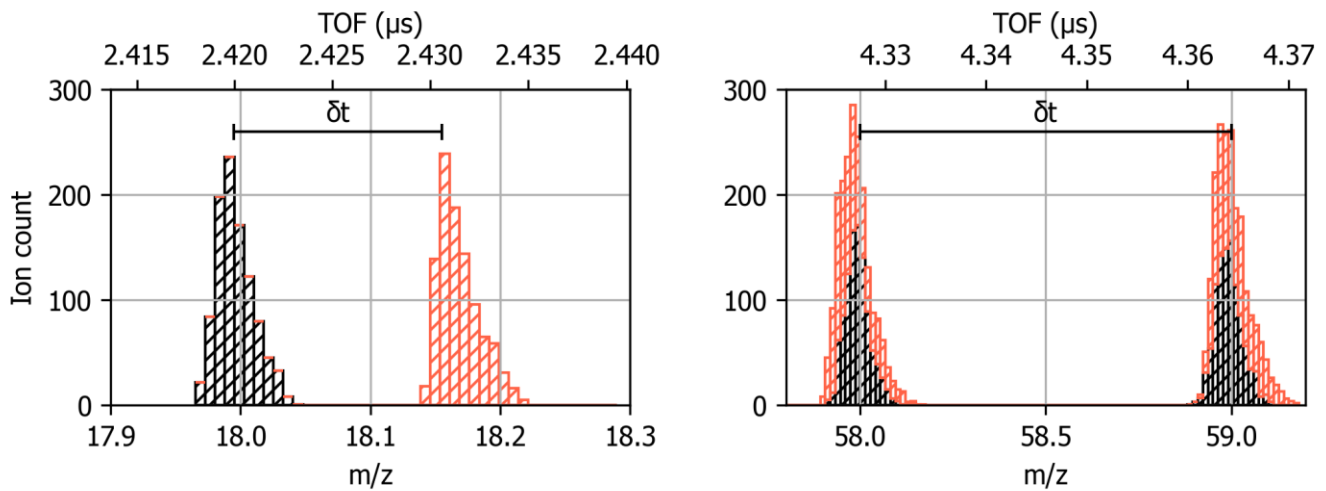


Figure 5. Simulated mass spectra of ions encountered at 20 km/s (black) and thermal velocities (orange) using a voltage set optimized for 20 km/s. For easier interpretation, flight times are converted to an m/z scale using mass calibration to the 20 km/s population. Left: $[\text{H}_2\text{O}]^+$ ions at m/z 18. Right: Ambient gas peaks at m/z 58 and 59 overlapping with thermal peaks of m/z 57 and 58, respectively.

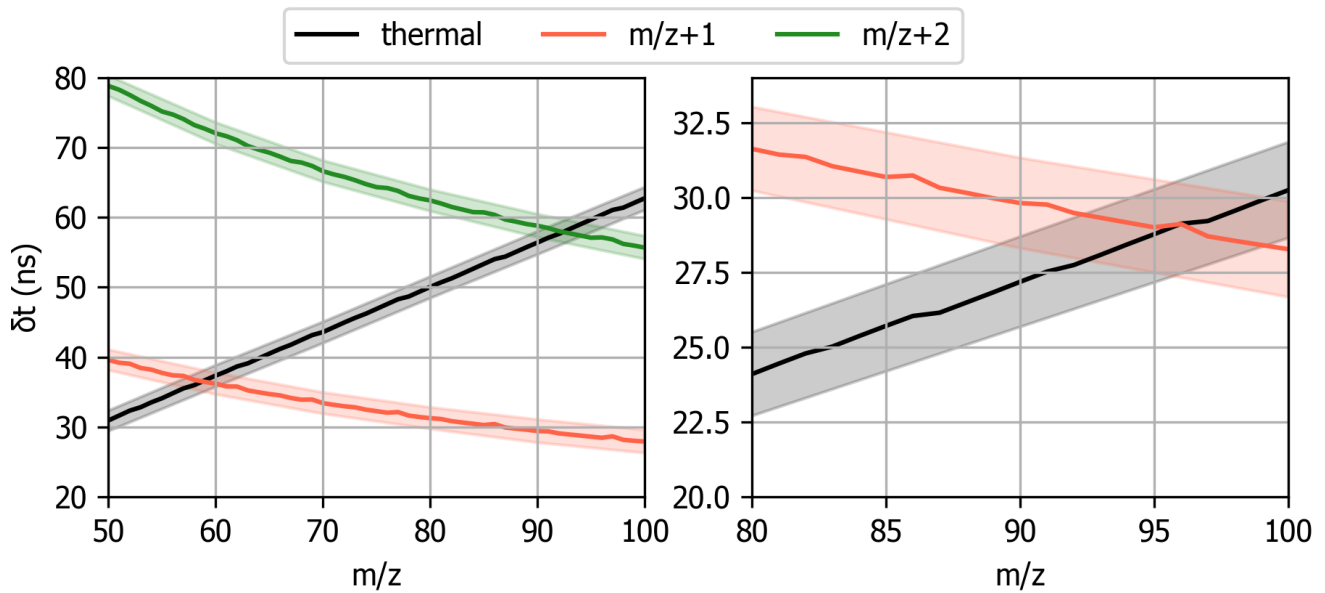


Figure 6. Flight time difference δt between ions encountered at flyby velocity and thermal velocities (black) compared to the time interval to the next two ambient gas mass packets (orange & green). Shaded regions indicate peak widths. Left: $v_{\text{rel}} = 20$ km/s. Right: $v_{\text{rel}} = 10$ km/s.

instrument at flyby speed provides these ions with a head start compared to ions which are accelerated from thermal velocities. Consequently, the flight times of the two populations differ as well. This difference in flight time δt increases with m/z . Thus, the two superposed mass spectra are slightly distorted. In Figure 5, two simulated mass spectra illustrate this flight time difference. The left-hand panel shows an exemplary mass spectrum of 1,000 $[\text{H}_2\text{O}]^+$ ions encountered each at a relative velocity of 20 km/s and with a thermal velocity distribution, respectively. At m/z 18, $[\text{H}_2\text{O}]^+$ is the predominant signal originating from spacecraft outgassing [20]. With peak widths (FWHM) around 3 ns and a δt of about 10 ns, the two peaks of water ions encountered at 20 km/s and at thermal velocities are clearly separated in time. Because the increase of δt with m/z is faster than that of the time interval between adjacent integer m/z mass peaks, there will be a region in the mass spectrum where the two are similar and the thermal mass peak overlaps with the next heavier ambient gas peak. In the right-hand panel of Figure 5, it is shown that thermal ions of m/z 57 and 58 catch up with ambient gas species of m/z 58 and 59, respectively, leading to overlapping signals. At higher m/z , there will also be a region where thermal ions catch up with the ambient gas ions with an m/z larger by two. The locations of these overlap regions in the mass spectrum depend on the relative encounter velocity. Figure 6 shows the increase of δt with increasing m/z and compares it to the corresponding time interval between subsequent mass packets of the ambient gas population encountered at flyby speed, which is 20 km/s in the left-hand panel and 10 km/s in the right-hand panel. With the shaded regions indicating the FWHM of the mass peaks, ambient gas and background signals interfere with each other where the shaded regions overlap. At 20 km/s, the affected regions are between m/z 55 and 62 as well as m/z 89 and 96.

For an encounter velocity of 10 km/s, mass peak overlap of thermal gas ions with ambient gas ions of adjacent m/z occurs between m/z 88 and 100. The region of overlap with ambient gas ions of $m/z+2$ is outside the mass range where significant background contamination is expected. For relative encounter velocities between 10 km/s and 20 km/s the regions of mass spectrum overlap are located between the two shown examples.

As can be seen, the relative encounter velocity dependent flight time allows a clear and unambiguous separation of ambient gas and spacecraft outgassing in the recorded mass spectra for the first time. To distinguish between the two contributions inside the narrow overlap regions, peak fitting routines can take advantage of the differing peak widths and shapes of the two populations to separate their respective signals. Monitoring of the spacecraft background during transit or sampling just prior to the flyby for optimization of peak fitting routines is also easily feasible without the need for spacecraft maneuvers. This is a marked advantage over current instruments, which have no capability of directly separating outgassing background from their intended measurements.

4. CONCLUSION

We presented the development of OpenTOF, a time-of-flight mass spectrometer that uses a novel gas inlet system to reliably analyze the composition of exospheres or plumes during hypervelocity flybys exceeding 5 km/s and up to 20 km/s. As opposed to previous instruments, it avoids surface contact of the analyzed species to prevent HVI induced molecular fragmentation. Due to the dependence of both mass resolution and flight time on the relative velocity

with which species are encountered, the instrument also provides the capability to separate the contamination originating from spacecraft outgassing from the desired ambient gas measurements. Intended for deep space missions, OpenTOF is unique in its capability of reliably and unambiguously analyzing complex molecules at high encounter velocities in the presence of spacecraft outgassing. Its novel features define a new state-of-the-art to search for complex (bio-) chemistry in tenuous upper atmospheres and plumes in deep space.

REFERENCES

- [1] S. M. MacKenzie *et al.*, “Science Objectives for Flagship-Class Mission Concepts for the Search for Evidence of Life at Enceladus,” *Astrobiology*, vol. 22, no. 6, pp. 685–712, Jun. 2022, doi: 10.1089/ast.2020.2425.
- [2] P. Wurz *et al.*, “Measurement of Io’s Atmosphere During The IVO Mission,” *52nd Lunar and Planetary Science Conference*, no. 1407, pp. 1–2, 2021, [Online]. Available: <https://www.hou.usra.edu/meetings/lpsc2021/pdf/1407.pdf>
- [3] B. Buffington and N. Strange, “Science-driven design of enceladus flyby geometry,” *AIAA 57th International Astronautical Congress, IAC 2006*, vol. 7, pp. 4478–4487, 2006, doi: 10.2514/6.iac-06-c1.6.05.
- [4] S. McEwen, L. P. Keszthelyi, K. E. Mandt, and the IVO Team, “The Io Volcano Observer (IVO),” *52nd Lunar and Planetary Science Conference*, no. 1352, pp. 1–2, 2021, [Online]. Available: <https://www.hou.usra.edu/meetings/lpsc2021/pdf/1352.pdf>
- [5] R. G. Fausch, J. A. Schertenleib, and P. Wurz, “Advances in Mass Spectrometers for Flyby Space Missions for the Analysis of Biosignatures and Other Complex Molecules,” *Universe*, vol. 8, no. 8, p. 416, Aug. 2022, doi: 10.3390/universe8080416.
- [6] W. C. Wiley and I. H. McLaren, “Time-of-flight mass spectrometer with improved resolution,” *Review of Scientific Instruments*, vol. 26, no. 12, pp. 1150–1157, 1955, doi: 10.1063/1.1715212.
- [7] A. Radionova, I. Filippov, and P. J. Derrick, “In pursuit of resolution in time-of-flight mass spectrometry: A historical perspective,” *Mass Spectrom Rev*, vol. 35, no. 6, pp. 738–757, Nov. 2016, doi: 10.1002/mas.21470.
- [8] Z. Ren *et al.*, “A review of the development and application of space miniature mass spectrometers,” *Vacuum*, vol. 155, pp. 108–117, Sep. 2018, doi: 10.1016/j.vacuum.2018.05.048.
- [9] J. H. Waite *et al.*, “The Cassini Ion and Neutral Mass Spectrometer (INMS) investigation,” *Space Sci Rev*, vol. 114, no. 1–4, pp. 113–231, Dec. 2004, doi: 10.1007/S11214-004-1408-2/METRICS.
- [10] H. Balsiger *et al.*, “Rosina - Rosetta orbiter spectrometer for ion and neutral analysis,” *Space Sci Rev*, vol. 128, no. 1–4, pp. 745–801, May 2007, doi: 10.1007/s11214-006-8335-3.
- [11] A. O. Nier, W. E. Potter, D. R. Hickman, and K. Mauersberger, “The open-source neutral-mass spectrometer on Atmosphere Explorer-C, -D, and -E,” *Radio Sci*, vol. 8, no. 4, pp. 271–276, 1973, doi: 10.1029/RS008I004P00271.
- [12] S. Meyer, M. Tulej, and P. Wurz, “Mass spectrometry of planetary exospheres at high relative velocity: Direct comparison of open- and closed-source measurements,” *Geoscientific Instrumentation, Methods and Data Systems*, vol. 6, no. 1, pp. 1–8, Jan. 2017, doi: 10.5194/GI-6-1-2017.
- [13] M. Föhn *et al.*, “Description of the Mass Spectrometer for the Jupiter Icy Moons Explorer Mission,” *2021 IEEE Aerospace Conference*, pp. 1–14, Mar. 2021, doi: 10.1109/AERO50100.2021.9438344.
- [14] T. G. Brockwell *et al.*, “The MAss Spectrometer for Planetary EXploration (MASPEX),” *2016 IEEE Aerospace Conference*, pp. 1–17, 2016, doi: 10.1109/AERO.2016.7500777.
- [15] C. Snodgrass and G. H. Jones, “The European Space Agency’s Comet Interceptor lies in wait,” *Nat Commun*, vol. 10, no. 1, Dec. 2019, doi: 10.1038/s41467-019-13470-1.
- [16] P. Wurz *et al.*, “Calibration Techniques,” *ISSI Scientific Reports Series*, vol. 7, pp. 117–276, Jan. 2007.
- [17] Z. Ulibarri *et al.*, “Detection of the amino acid histidine and its breakup products in hypervelocity impact ice spectra,” *Icarus*, vol. 391, p. 115319, Feb. 2023, doi: 10.1016/J.ICARUS.2022.115319.
- [18] A. Jaramillo-Botero, M. L. Cable, A. E. Hofmann, M. Malaska, R. Hodyss, and J. Lunine, “Understanding Hypervelocity Sampling of Biosignatures in Space Missions,” *Astrobiology*, vol. 21, no. 4, pp. 421–442, Apr. 2021, doi: 10.1089/ast.2020.2301.
- [19] V. R. Haemmerle and J. H. Gerhard, “Cassini Camera Contamination Anomaly: Experiences and Lessons Learned,” *SpaceOps 2006 Conference*, 2006.
- [20] B. Schläppi *et al.*, “Influence of spacecraft outgassing on the exploration of tenuous atmospheres with in situ mass spectrometry,” *J. Geophys. Res*, vol. 115, p. 12313, 2010, doi: 10.1029/2010JA015734.
- [21] R. G. Fausch, J. A. Schertenleib, and P. Wurz, “Reliably Analyzing the Chemical Composition of Plumes during Flybys at Velocities Exceeding 5 km/s,” *2023 IEEE Aerospace Conference*, pp. 1–8, Mar. 2023, doi: 10.1109/AERO55745.2023.10115795.
- [22] R. Fausch, P. Wurz, B. Cotting, U. Rohner, and M. Tulej, “Direct Measurement of Neutral Gas during Hypervelocity Planetary Flybys,” *2022 IEEE Aerospace Conference*, pp. 1–12, 2022, doi: 10.1109/AERO53065.2022.9843767.
- [23] R. Fausch, M. Föhn, S. Meyer, P. Wahlström, S. Wyler, and P. Wurz, “Power-Efficient Electron Emitters for Electron Ionization in Spaceborne Mass

Spectrometers,” 2024 IEEE Aerospace Conference (submitted).

- [24] B. A. Mamyryn, V. I. Karataev, D. V. Shmikk, and V. A. Zagulin, “The mass-reflectron, a new nonmagnetic time-of-flight mass spectrometer with high resolution,” *Soviet Journal of Experimental and Theoretical Physics*, vol. 37, p. 45, 1973, Accessed: Mar. 20, 2023. [Online]. Available: <https://ui.adsabs.harvard.edu/abs/1973JETP...37...45M>
- [25] A. Bieler *et al.*, “Optimization of mass spectrometers using the adaptive particle swarm algorithm,” *Journal of Mass Spectrometry*, vol. 46, no. 11, pp. 1143–1151, Nov. 2011, doi: 10.1002/jms.2001.

BIOGRAPHY



Janis Schertenleib obtained his Bachelor’s degree in Physics in 2021 and his Master’s degree in Experimental Physics in 2023, both from the University of Bern (Switzerland) in 2021. For his Master’s thesis, he worked at the Space Science and Planetology division, designing and testing ion-optical systems for time-of-flight mass spectrometers. After graduating, he joined the Spacetek Technology AG, Switzerland, where he develops mass spectrometers.



Rico Fausch completed an apprenticeship as a mechanical design engineer before he received a B.Sc. in Systems Engineering (micro technologies) from NTB University of Applied Science (Switzerland) in 2013 and an M.Sc. in Biomedical Engineering from University of Bern (Switzerland) in 2015. He has been with the Physics Institute of the University of Bern since 2016, where he received his Ph.D. in Physics in 2020 for the finalization of the NGMS/Luna-Resurs. As a post-doctoral researcher, he is involved in the design of several space missions and space instrumentation including NIM/JUICE.



Peter Wurz has a degree in electronic engineering (1985), an M.Sc. and a Ph.D. in Physics from Technical University of Vienna (1990). He has been a post-doctoral researcher at Argonne National Laboratory. At the University of Bern since 1992, he is a professor of physics, since 2015 head of the Space Science and Planetology division, and since 2022 director of the Physics institute. He has been Co-I and PI for many science instruments for space missions of ESA, NASA, ISRO, Roscosmos, and JAXA. He is PI of NIM and Co-PI of PEP on board JUICE.